ISIJ International, Vol. 63 (2023), No. 2, pp. 382–389
https://doi.org/10.2355/isijinternational.ISIJINT-2022-365

Effect of Tempforming Temperature on the Impact Toughness of an HSLA Steel

Anastasiia DOLZHENKO,[1)] Andrey BELYAKOV[1)]* and Rustam KAIBYSHEV[2)]

1) Belgorod State University, Belgorod, 308015 Russia.
2) Russian State Agrarian University—Moscow Timiryazev Agricultural Academy, Moscow, 127550 Russia.

(*Received on August 16, 2022; accepted on October 26, 2022*)

The fracture behavior of a high-strength low-alloy steel subjected to tempforming at 873 K, 923 K, or 973 K was studied by means of impact and bending tests. A decrease in tempforming temperature promoted the grain refinement resulting in the ultrafine grained lamellar-type microstructure with finely dispersed particles that led to significant strengthening along with an increase in the impact toughness. The tempformed steel samples exhibited Charpy V-notch impact energy well above 100 J at temperatures of 183–293 K due to delamination along the rolling plane during bending, which was attributed to high anisotropy of cleavage fracture stress. Delamination owing to easy cleavage crosswise to the impact direction blunted the primary crack and resulted in the zigzag crack propagation, leading to high impact toughness. Depending on tempforming temperature, three types of the delamination behavior were observed in the V-notch specimens upon three-point bending tests at room temperature. Namely, the early, restrained, and late delaminations took place in the samples after tempering at 873 K, 923 K, and 973 K, respectively. On the one hand, a decrease in the test temperature promoted delamination, and on the other the strengthening by lowering tempforming temperature is accompanied by a suppression of ductile fracture. The sample tempformed at 873 K exhibited the highest impact toughness at room temperature, whereas the samples tempformed at 923–973 K were characterized by the higher impact toughness at 183–233 K.

KEY WORDS: high-strength low-carbon steel; tempforming; ultrafine grained microstructure; strengthening; impact toughness.

1. Introduction

One of the significant drawbacks of high-strength low-alloy (HSLA) steels is a relatively high temperature of ductile to brittle transition that significantly limits their usage at lowered temperatures.[1)] This stimulates materials scientists to enhance their efforts on finding the promising approaches to strengthen the steels without degradation of the impact toughness. Comprehensive studies of the fracture mechanisms and the conditions of the ductile-brittle transition have being carried out from the middle of the last century.[2–4)] The first successes in the creation of tough steels were associated with an increase in the alloying extent, mainly nickel. The detailed studies using electron microscopy revealed that such alloying led to an increase in the probability of ductile fracture.[5)] A great attention was paid to thermal and thermo-mechanical treatments in combination with the modification of the chemical composition of low-alloyed steels in order to obtain a specific microstructure, which should provide a high level of strength and toughness. The Yoffee diagram suggests two possible ways to suppress a ductile-brittle transition.[1)] Those are increasing the cleavage resistance or decreasing the effective flow stress. An intergranular embrittlement frequently results from segregations of sulfur and phosphorus at grain boundaries. Thus, the steel purification is used to remove harmful impurities or micro-alloying is applied to involve harmful impurities into mechanically safe precipitations.[1)] The resistance to transcrystalline fracture can be increased owing to reducing the effective grain size, which leads to a reduction of the free path of crack propagation. Several methods have been developed for grain refinement, including thermo-mechanical processing of ingots into strips, sheets or rods,[6)] and thermal cycling manipulating phase transformations during quenching or tempering in order to provide the uniform dispersion of nano-sized secondary phase particles.[7)]

A promising approach to increase the impact toughness at lowered temperatures was proposed by Japanese scientists.[8)] This approach consists in the formation of an ultrafine grained lamella-type microstructure with a homogeneous distribution of finely dispersed nanoscale particles of secondary phases by means of warm rolling under con-

* Corresponding author: E-mail: belyakov@bsu.edu.ru

ditions of tempering. Such thermo-mechanical processing method, tempforming, results in a promising combination of mechanical properties in low-alloy steels.[9–11] The dispersion strengthened ultrafine grained microstructure provides high strength. On the other hand, the lamellar microstructure delaminates along the rolling plane, thereby blunting the original crack and increasing the impact toughness for crack arrestor orientation. This phenomenon was called delamination toughness. It should be noted that tempforming of medium carbon steels simultaneously leads to hardening and an increase in toughness, which in some cases showed an inverse temperature dependence that is quite unusual for carbon steels.[10,11] Lowering the temperature of tempforming leads to an increase in the strength and hardly affects the toughness of medium carbon steels.[9] As compared to conventional tempering, however, a decrease in tempforming temperature improves substantially the impact toughness.[9] Recently, an excellent combination of impact toughness and hydrogen embrittlement was achieved by Kimura *et al.* in a high-strength medium carbon steel by tempforming at relatively low temperature.[12] Although tempforming can significantly increase the strength and toughness of carbon steels, its effectiveness decreases with increasing carbon content from 0.2 to 0.6%.[11] Hence, high-strength low-alloy steels with a carbon content below 0.2% seem to be the most appropriate candidates for tempforming in order to improve their mechanical performance. Advances of tempforming over ausforming for HSLA steels were recently confirmed.[13] An important role of dislocation strengthening was clarified for a HSLA steel.[14] However, the regularities of delamination toughness, their dependence on tempering time, temperature, and strain are still unclear. A decrease in tempforming temperature was shown to promote the impact toughness of medium carbon steels at room and lowered temperatures, whereas tempforming at a relatively high temperature increased the impact toughness at the cryogenic temperature.[15,16] An increase in total strain during tempforming of a medium carbon steel also improved the impact toughness, especially, at cryogenic temperatures,[15] although the mechanisms controlling such behavior were not detailed. A deep knowledge of the microstructural dependence of the fracture behavior for HSLA steels subjected to warm rolling is of crucial importance for tempforming implementation to produce advanced structural materials. The aim of the present study, therefore, is to clarify the delamination toughness behavior of an HSLA steel subjected to tempforming at different temperatures.

2. Experimental

A steel with a chemical composition of Fe–0.08C–0.17Si–1.16Cr–1.55Mn–0.03Nb–0.005Al–0.42Mo–0.08V–0.003B–0.003P–0.006S (all in mass%) was selected as a promising representative of advanced HSLA steels with a strength of well above 700 MPa after conventional tempering. The steel samples were quenched from 1 373 K and tempered for 1 h at 873 K or 923 K or 973 K followed by plate rolling without lubrication at the same temperature to a total strain of 1.5 (thickness reduction from 45 mm to 10 mm). The steel samples were reheated to the designated temperature before each rolling pass comprising about 20% reduction. The tempformed microstructures were observed on the longitudinal sections normal to the transverse direction (TD), using a Quanta Nova Nanosem 450 scanning electron microscope (SEM) equipped with an electron back scattering diffraction pattern (EBSP) analyzer incorporating an orientation imaging microscopy (OIM) system. The OIM images were subjected to cleanup procedure setting minimal confidence index of 0.1. The grain size was evaluated by the linear intercept method on the OIM images as an average distance between high-angle boundaries (HAB) with misorientations of $\theta \geq 15°$. Standard Charpy V-notch specimens were tested using an Instron 450 J impact machine with an Instron Dynatup Impulse data acquisition system at temperatures ranging from 183 K to 293 K. The specimens for impact tests were cut from the rolled plates so that the impact direction was parallel to the normal direction (ND), *i.e.*, the crack-arrestor orientation.[17] The three-point bending tests of Charpy V-notch specimens were carried using an Instron 5 882 testing machine at a room temperature with a crosshead speed of 2 mm/min.

3. Results

3.1. Tempformed Microstructures

The representative microstructures evolved in the steel subjected to tempforming at different temperatures are shown in **Fig. 1**. The developed microstructures and textures were detailed elsewhere[14] and can be briefly introduced here as follows. The tempformed microstructures consist of flattened grains that are highly elongated along RD. An average grain size measured along ND varies from 350 nm

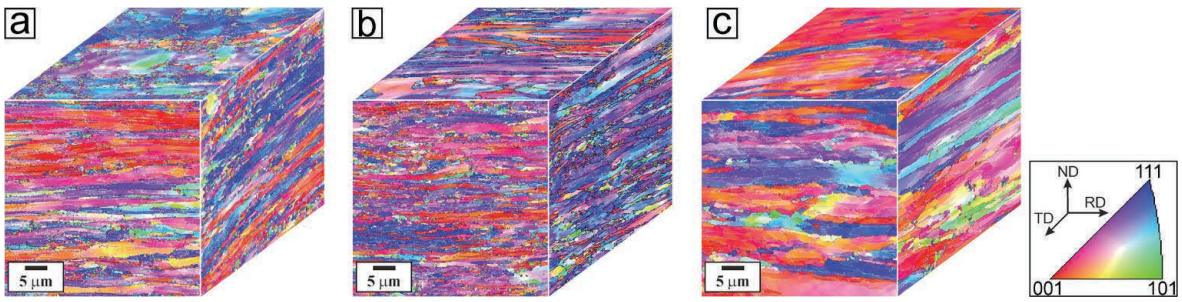

Fig. 1. Microstructures developed in an HSLA steel subjected to tempforming at 873 K (a), 923 K (b) and 973 K (c). Colours correspond to the crystallographic direction along the normal direction (ND). The black and white lines indicate high-angle boundaries ($\theta \geq 15°$) and low-angle sub-boundaries ($2° \leq \theta < 15°$), respectively. (Online version in color.)

Table 1. Effect of tempforming temperature (T_{TF}) on the transverse grain size (D), an average size (d) and the volume fraction (F_V) of relatively coarse $Cr_{23}C_6/Fe_3C$ particles and finely dispersed NbC/VC particles.

T_{TF}, K	D, nm	d($Cr_{23}C_6/F_3C$), nm	F_V($Cr_{23}C_6/F_3C$), %	d(NbC/VC), nm	F_V(NbC/VC), %
873	350 ± 50	40 ± 8	0.85	4 ± 1	0.129
923	630 ± 50	50 ± 10	0.91	7 ± 1.5	0.133
973	950 ± 50	90 ± 20	0.94	17 ± 3	0.135

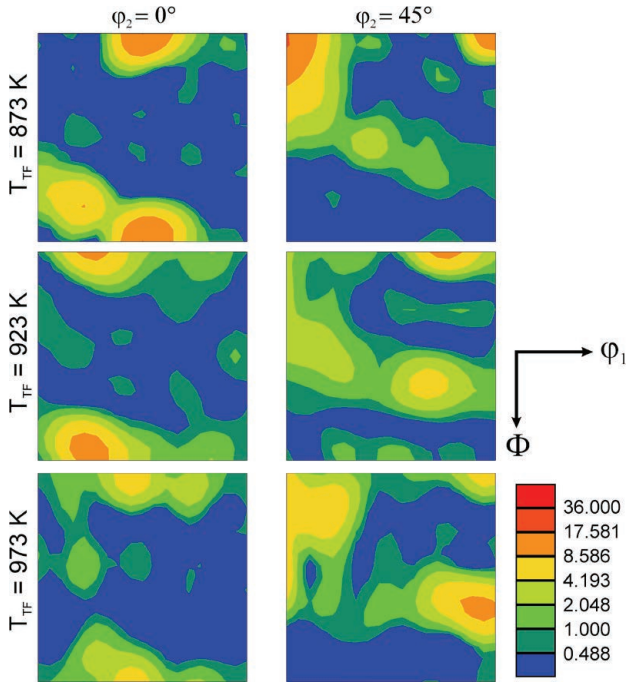

Fig. 2. The sections of orientation distribution functions (ODF) at $\varphi_2 = 0°$ and $\varphi_2 = 45°$ for an HSLA steel subjected to tempforming at different temperatures (TTF). (Online version in color.)

to 950 nm, depending on tempforming temperature. The dispersed particles are represented by rather coarse $Cr_{23}C_6$ and Fe_3C carbides located at grain/subgrain boundaries and fine (Nb,V)C carbides uniformly distributed throughout. The size of former ones increases from 40 nm to 90 nm and that of the latter ones increases from 4 nm to 17 nm with an increase in tempforming temperature. Correspondingly, the number density of carbide particles decreases with an increase in processing temperature. Some parameters of the tempformed microstructures are represented in **Table 1**. Commonly, the texture evolved after tempforming consists in partial α-fiber (<110>//RD), η-fiber (<100>//ND), and γ-fiber (<111>//ND), including strong {001}<110> and {111}<110> components (**Fig. 2**) that have been frequently observed in plate-rolled bcc-metals/alloys.[18,19] An increase in tempforming temperature weakens the texture as discussed in previous study.[14] Rather strong {011}<110> (Rotated Goss) and {001}<110> (Rotated Cube) texture components were observed by Inoue *et al.* from the side direction in low carbon steel subjected to caliber warm rolling to large strains owing to rotation of the rolled bar by 90° in each rolling pass.[20] Since the side direction is just between the normal and transverse ones in the plate rolling, strong {223}<110> and {111}<110> components that located on α-fiber between {011}<110> and {111}<110> should be expected in the present samples. Relatively weak corresponding texture components in the present study as compared to previous one[20] may result from smaller total strain (less than half) applied in the present plate rolling.

3.2. Mechanical Tests

3.2.1. Impact Toughness

The load – displacement curves and the corresponding effect of test temperature on the impact toughness are shown in **Figs. 3** and **4**, respectively. The impact toughness of the same steel subjected to modified ausforming[13] is also indicated in Fig. 4 for comparison. Irrespective of the test temperature, the shape of the impact load – displacement curves in Fig. 3 remarkably depends on the tempforming temperature. Following the general yield the load increases to its maximum followed by a gradual decrease until a drastic drop to almost zero during the impact tests of the steel samples tempformed at 873 K (Fig. 3(a)). Note here that the tiny serrations can be observed at general yield. A decrease in the test temperature does not lead to remarkable changes in the general yield and maximal loads. In contrast, the stage of gradual decrease in the load that is associated with the stable crack propagation shortens and the complete fracture occurs at smaller displacements with a decrease in test temperature. Thus, the absorbed energy for these specimens decreases from about 450 J/cm^2 to 120 J/cm^2 with a decrease in test temperature from 293 K to 213 K (Fig. 4).

Similar to tempforming at 873 K, the impact load – displacement curves for the samples tempformed at 923 K are characterized by a gradual increase in the load to its maximum at rather large displacements followed by steadily decreasing the load until a sudden drop, although their impact toughness is higher at all test temperatures (Fig. 3(b)). Two main differences should be highlighted for the impact specimens made of steel tempformed at 923 K comparing to those tempformed at 873 K. Namely, the tiny serrations at yielding point are more visible irrespective of test temperature and the type of crack-arrester behavior takes place upon tests at 233–293 K. Following the crack-arrest the load gradually decreases as the displacement increases up to 30 mm, when the specimens are pushed out from the holder. Therefore, the steel samples tempformed at 923 K are characterized by the high impact toughness above 400 J cm^{-2} at 233–293 K (Fig. 4). Further decrease in tests temperature to 183 K is accompanied by a decrease in the impact toughness to about 300 J cm^{-2}.

The impact load – displacement curves obtained for the steel samples after tempforming at 973 K are quite different from those after tempforming at 873–923 K. The steel samples processed at the highest tempforming temperature of 973 K exhibit a well defined load drop after general yielding followed by a long stage of apparently stable crack

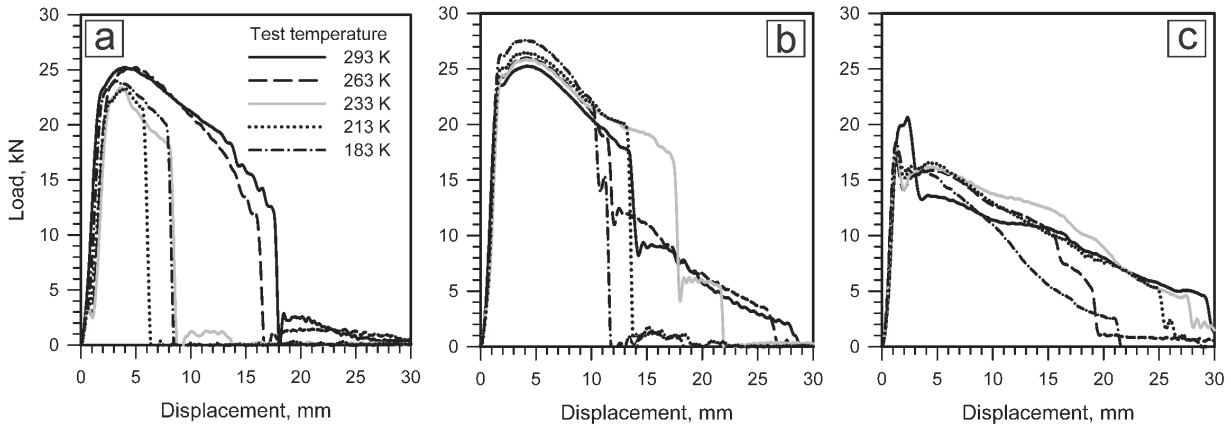

Fig. 3. Impact load vs displacement curves of an HSLA steel subjected to tempforming at 873 K (a), 923 K (b) and 973 K (c).

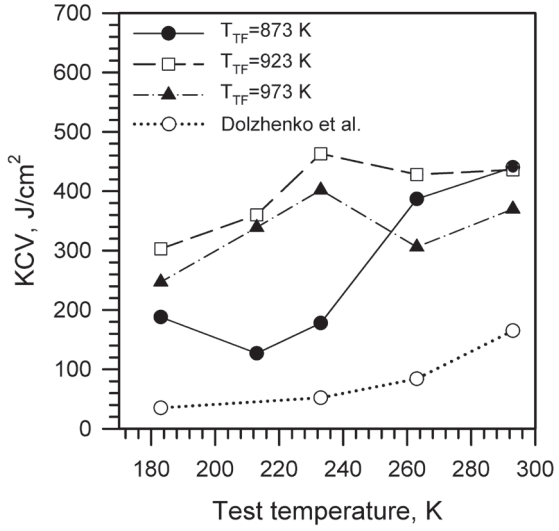

Fig. 4. Effect of test temperature on the impact toughness (KCV) of an HSLA steel subjected to tempforming at different temperatures (T_{TF}). The open cycles indicate KCV for the same steel after quenching and tempering.[13)]

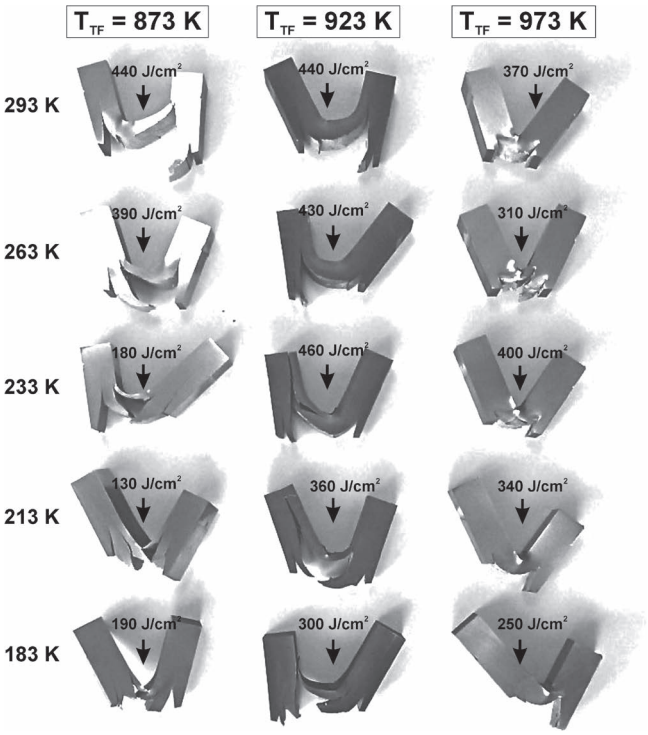

Fig. 5. Specimens of an HSLA steel tempformed at T_{TF} = 873 K, 923 K and 973 K and then subjected to impact tests at indicated temperatures.

propagation, when the impact load decreases to a very low value (Fig. 3(c)). The general yield is almost the same with the maximum load; and these both have relatively low values. Therefore, the absorbed energy during the impact tests of the steel samples tempformed at 973 K is somewhat lower than that for the samples processed at 923 K.

The general view of the specimens after impact tests is shown in **Fig. 5**. The impact tests are accompanied by delamination of highly bent specimens without their complete rupture that suggest very high absorbed impact energy. Therefore, the steel subjected to tempforming at 873–973 K exhibits well-defined delamination toughening[8,21)] at test temperatures of 183–293 K. The primary transverse crack propagating directly across the central portions of the specimens branches along the rolling plane. Then, the secondary cracks growing across the specimens again may experience branching towards RD leading to the next delamination event as clearly seen in Fig. 5 for the specimens after tempforming at temperatures (T_{TF}) of 873–923 K. Hence, the largely bent delaminated specimens without complete separation are observed after impact tests. A decrease in tempforming temperature from 973 K to 923 K remarkably promotes delamination, whereas further decrease of T_{TF} to 873 K has a marginal effect on delamination irrespective of test temperature.

Representative SEM images of the fracture surfaces after impact tests at 293 K and 183 K are shown in **Figs. 6** and **7**, respectively. The fracture surfaces that resulted from the crack propagation along the impact direction are distinctly different from those caused by the crack propagation perpendicular to the impact direction. It is seen that primary macrocrack propagates directly across the central portions of the impact test bars in ductile manner (left-side pictures in Fig. 6). The propagation of primary crack is arrested by crack tip blunting owing to huge cleavage along the rolling plane (right-side pictures in Fig. 6). This is typical for the delamination toughness phenomenon, when the easy cleavage crosswise to the impact direction prevents the

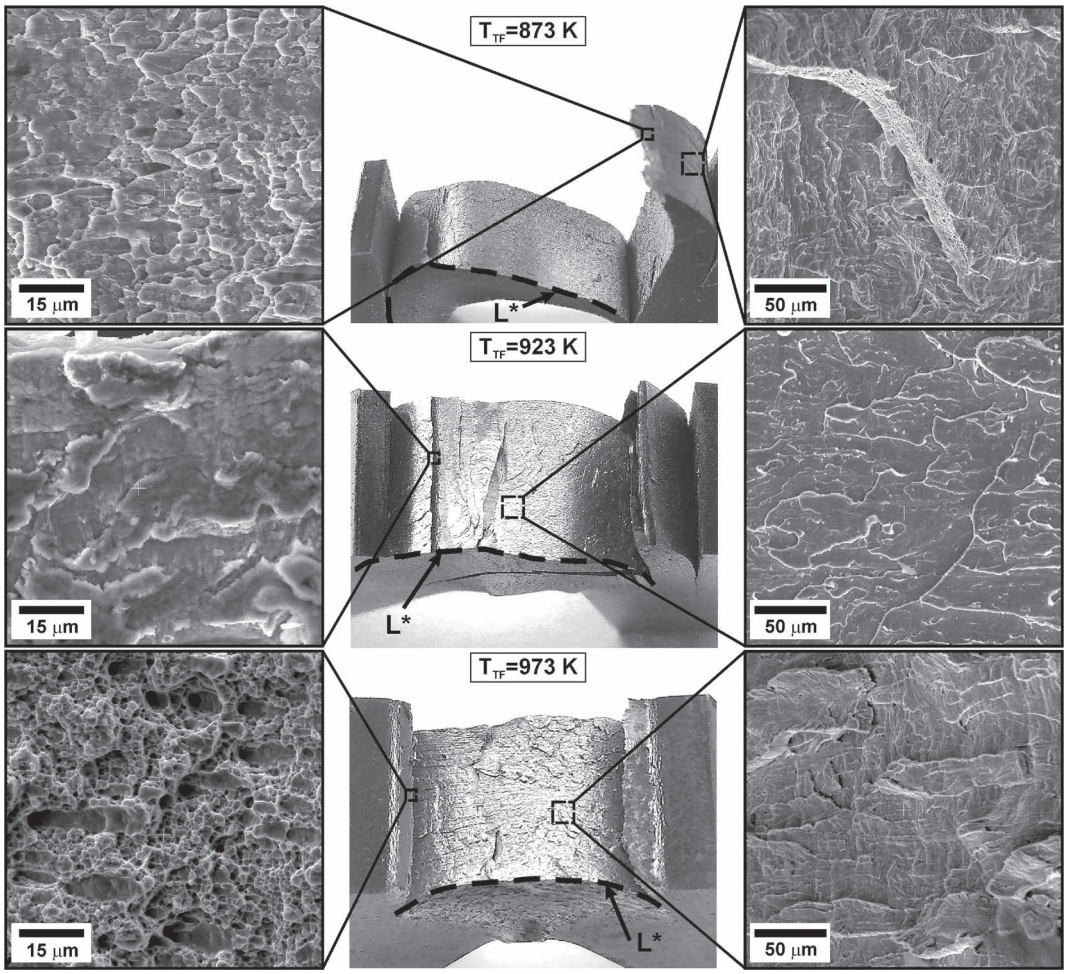

Fig. 6. Fracture surfaces after impact tests at 293 K of an HSLA steel tempformed at temperatures (T_{TF}) of 873 K, 923 K and 973 K.

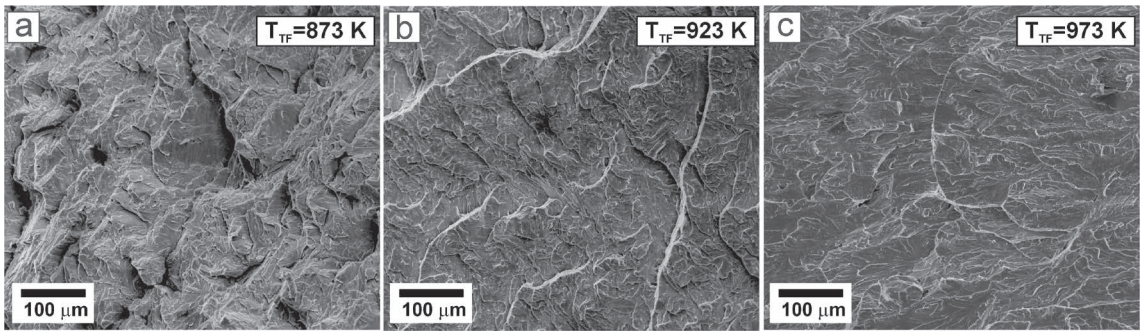

Fig. 7. Fracture surfaces after impact tests at 183 K of an HSLA steel subjected to tempforming at T_{TF} = 873 K (a), 923 K (b) and 973 K (c).

crack propagation along the impact direction and, therefore, enhances the impact toughness owing to increasing the absorbed energy.[21,22] The longitudinal delaminating cracks propagate over a large distance indicated by L* (center pictures in Fig. 6), leading to the broad fracture surface consisting of terraces with lateral dimple fracture surfaces. A decrease in test temperature does not significantly affect the fracture behavior. The height of terraces, *i.e.*, the dimensions of the fracture surfaces crosswise to the delaminating planes, apparently decreases (cf. Figs. 6 and 7), reducing the total ductile fracture surface and, therefore, decreasing the impact toughness.

3.2.2. Three-Point Bending

The three-point bending tests reveal three distinctive fracture behavior in the present steel samples, depending on the temperature of tempforming (**Figs. 8** to **10**). The load – displacement curve for the steel specimen after tempforming at 873 K is shown in Fig. 8 along with some characteristic side-views on the bent specimen. Small cracks running crosswise to the loading direction seem to appear before general yielding. It should be noted that following the early cracking the crack propagation along the specimen (delamination) during further bending may be accompanied by a gradual increase in the load. On the other hand, the rapid expansion of pre-existing crack over a large distance

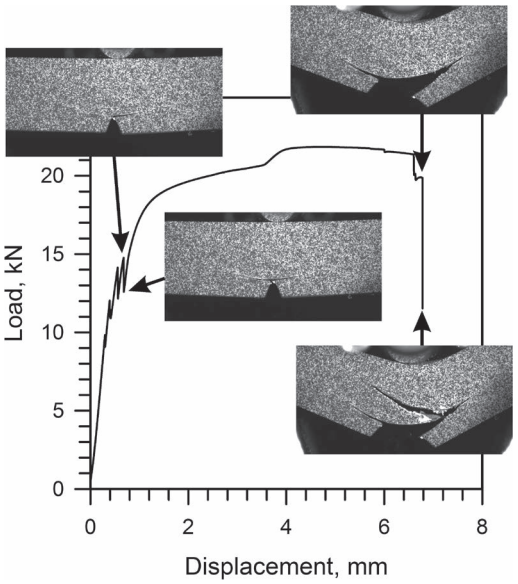

Fig. 8. Bending load – displacement curves and characteristic side-views of bent specimen of an HSLA steel subjected to tempforming at 873 K.

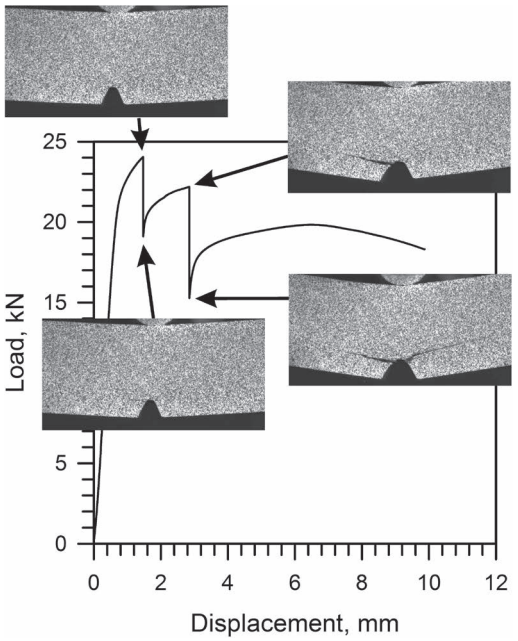

Fig. 9. Bending load – displacement curves and characteristic side-views of bent specimen of an HSLA steel subjected to tempforming at 923 K.

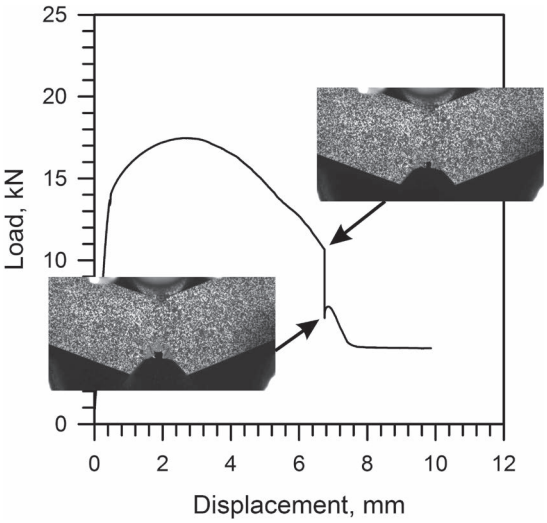

Fig. 10. Bending load – displacement curves and characteristic side-views of bent specimen of an HSLA steel subjected to tempforming at 973 K.

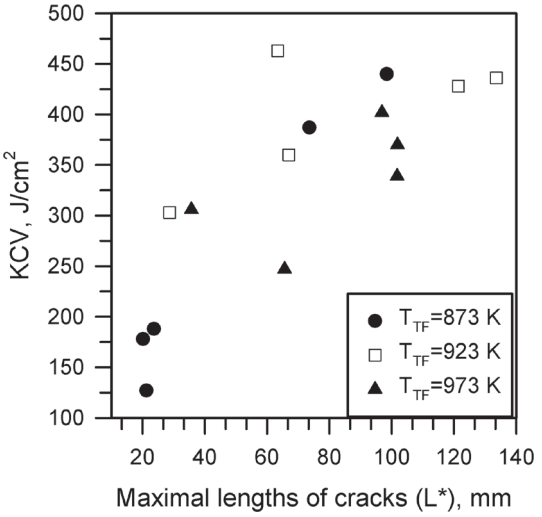

Fig. 11. Relationship between the maximal lengths of delaminating cracks (L*) along the impact specimens (s. Fig. 6) and the impact toughness of an HSLA steel subjected to tempforming at different temperatures (T_{TF}).

results in distinctive serration on the bend curve. The specimen with the longitudinal cracks can be characterized by a long stage of strain hardening upon bending over a large angle corresponding to a displacement of approx. 5 mm in Fig. 8. Then, the next occurrence of huge delaminating crack leads to substantial drop of the load at the bend curve. Such sequential formation of the longitudinal cracks (delamination) finally results in zigzag-type fracture of the highly bent specimen.

The steel sample subjected to tempforming at 923 K exhibits another type of fracture behavior upon the bending tests (Fig. 9). The first cracking crosswise to the loading direction occurs at the stage of strain hardening after the general yield. Then, the bend load increases continuing the strain hardening stage followed by the next cracking (delamination) at rather large displacement (2 mm in Fig. 9). The bend load attains the maximal value at a displacement of about 6 mm in Fig. 9 much similar to that for the specimen after tempforming at 873 K. Further bending over a large displacement is accompanied by a progressive expansion of the pre-existing delaminating cracks. Quite different bending fracture behavior is observed for the specimen after tempforming at 973 K (Fig. 10). The bend load increases to its maximum followed by gradual decrease due to small cracks growing across the specimen during bending to large displacement. Remarkable crack, which can be considered as a delamination beginning, appears at large displacements, *e.g.*, 6 mm in Fig. 10.

The strain rate in the three-point bending tests is much lower compared to that for impact tests. This makes possible to resolve the special features of fracture behavior

of the specimens with different microstructures evolved at different temperatures of tempforming. Although recovery processes during the three-point bending may delay and move the characteristic changes associated with the crack nucleation and propagation to larger strains as compared to impact tests as it was observed in previous study for the maximal and fracture loads,[23] the general fracture behavior should share some traits.

Thus, the fracture behavior of the V-notch specimens upon bending depends significantly on temperature of tempforming. A decrease in tempforming temperature promotes the cracking along the rolling plane, *i.e.*, delamination on planes that are perpendicular to the bend loading direction. The specimens after tempforming at relatively low temperature of 873 K are characterized by early delamination that blunts the notch, leading to strain hardening during bending over large angles. In contrast, the specimens after tempforming at rather high temperature of 973 K exhibit delayed delamination. Following the strain hardening at early stage of bend tests, these specimens begin to rupture due to small cracks developing towards the loading direction, *i.e.*, across the specimen, whereas delamination occurs at large bending. The steel samples subjected to tempforming at intermediate temperature of 923 K demonstrate transitional fracture behavior during bending. Namely, the delamination cracking occurs when the bend load approaches its maximum. Thus, the fracture of this specimen begins with delamination along the specimen similar to that after tempforming at 873 K, although the specimen experiences rather large plastic deformation before delamination like that after tempforming at 973 K.

4. Discussion

The present impact specimens are characterized by a remarkable delamination along the specimen, *i.e.*, across the impact direction (Fig. 5). Considering the stress state around the notch, the conditions for delamination have been discussed as a result of the difference between the cleavage stress crosswise the specimen (along the impact direction) and the plastic flow stress along the specimen that controls the specimen bending.[24] The development of the microstructure consisting in pan-caked grains highly elongated along the rolling direction as well as the large texture component of <100>//ND, which promotes the cleavage along the rolling plane, decreases the critical stresses for corresponding brittle fracture leading to pronounced delamination.[9] The relationship between the maximal lengths of delamination cracks (L* in Fig. 6) and the impact toughness is represented in Fig. 11. It is clearly seen that larger L* corresponds to higher KCV. Thus, the extraordinarily high impact toughness of the tempformed steel is closely connected with the delamination development. The temperature dependence of delamination has been discussed as a reason for unusual increase in the impact toughness with decreasing test temperature.[8] The yield stress increases while that for brittle fracture remains almost unchanged as the test temperature decreases that should promote delamination.

The delamination toughness was discussed referring to modified Yoffee diagram comparing the effective yield stress along the impact specimen, *i.e.*, along the rolling direction ($\sigma_{Y//RD}$) and the cleavage fracture stress crosswise to the specimen, *i.e.*, along the normal direction ($\sigma_{C//ND}$).[11,25] An increase in the impact toughness owing to delamination can be expected with a decrease in tests temperature to the range of $\sigma_{Y//RD} > \sigma_{C//ND}$ in **Fig. 12**(a). In this case the brittle fracture along the specimen readily occurs blunting the original crack and advancing the specimen bending over a large angle. The present results suggest that the tendency to delamination suppresses with an increase in tempforming temperature because of increasing $\sigma_{C//ND}$ and decreasing $\sigma_{Y//RD}$ (Fig. 12(a)). Indeed, the delamination occurs at larger load/displacement in the specimen tempformed at higher temperature (cf. Figs. 8 and 9). On the other hand, both the yield strength and the ultimate tensile strength significantly decreased from 1 230 MPa and 1 250 MPa, respectively, to 690 MPa and 760 MPa with an increase in tempforming temperature from 873 K to 973 K.[14] The fracture behavior in Figs. 8 and 9 suggests that the delamination of the steel specimens after tempforming at 873 K and 923 K is controlled by the load (stress-controlled delamination). An early delamination precedes the plastic deformation of the specimen tempformed at 873 K (Fig. 8), or occurs soon after general yield in the specimen tempformed at 923 K (Fig. 9). Tempforming temperature in the latter case can be considered as the range around the intersection point in Fig. 12(b), where $\sigma_{C//ND}$ and $\sigma_{Y//RD}$ are close to each other. In contrast, delamination of the specimen tempformed at 973 K takes

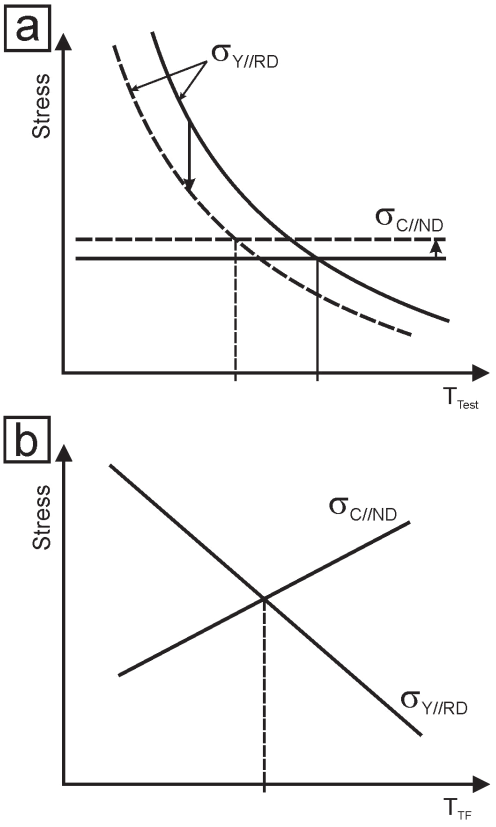

Fig. 12. Modified Yoffee diagram illustrating the effect of increasing tempforming temperature on the fracture behavior at different temperatures, T_{test}, (a) and variations of the cleavage fracture stress crosswise to the impact specimen, $\sigma_{C//ND}$, and the effective yield stress along the impact specimen, $\sigma_{Y//RD}$, with tempforming temperature, T_{TF}, (b).

place after large bending, when the specimen experienced rather large plastic deformation as well as a partial ductile fracture along the loading direction (Fig. 10). This can be considered as a deformation-controlled delamination; and the corresponding temperature of tempforming lies in the right to the intersection point in Fig. 12(b), where $\sigma_{C//ND} > \sigma_{Y//RD}$.

The consideration above suggests a promising approach to select the tempforming conditions. The highest impact toughness should be expected after tempforming at a temperature close to the intersection in Fig. 12(b). In the present study this temperature corresponds to about 923 K. It should be noted that the beneficial effect of tempforming on the impact toughness in this case is observed in a wide range of test temperatures down to 183 K. Tempforming at a lower temperature, *e.g.*, 873 K, facilitates delamination. However, easy delamination repeatedly occurring in the specimen processed at 873 K results in the fast zigzag fracture at relatively small displacements decreasing the impact toughness, especially, at relatively low temperatures. An increase in tempforming temperature results in delamination after remarkable plastic deformation followed by a large bending of specimen without completed fracture. Such processing may be useful for very low temperature applications, although relatively low strength after tempforming at elevated temperature limits the impact toughness, which ranks below that for the steel samples tempformed at optimal temperature.

5. Conclusions

Effect of tempforming (warm plate rolling following tempering) temperature in the range of 873–973 K on the impact toughness at 183 K to 293 K of a high-strength low-alloy steel was studied. The main results can be summarized as follows.

(1) Tempforming substantially enhanced the impact toughness, which was well above 100 J/cm^2 within the studied range of impact test temperatures. The high values of impact toughness resulted from delamination of the impact specimens crosswise to the loading direction. Rapid delamination by brittle fracture mode blunted the original crack and, hence, supported bending of the specimen over a large angle.

(2) The impact toughness at low temperatures of 183–263 K increased with an increase in tempforming temperature from 873 K to 923 K followed by a decrease with further increase in tempforming temperature to 973 K. Such variation in the impact toughness was attributed to the difference in the fracture behavior upon bending that changed from early to delayed delamination with an increase in tempforming temperature.

(3) The steel specimen after tempforming at 873 K experienced delamination during bending in the elastic deformation domain. Such easy delamination resulted in the fast repeated brittle crack propagation decreasing the impact toughness, especially, at low temperatures. In contrast, the specimen subjected to tempforming at 973 K is characterized by pronounced plastic deformation before delamination upon bending. However, relatively low strengthening at a high tempforming temperature diminished the beneficial effect of delamination on the impact toughness.

Acknowledgements

This study was financially supported by the Ministry of Science and Higher Education of the Russian Federation, Grant No. 075-15-2021-572. The work was carried out using the equipment of the Joint Research Center, Technology and Materials, of Belgorod State University.

REFERENCES

1) J. W. Morris, Jr.: *Science*, **320** (2008), 1022. https://doi.org/10.1126/science.1158994
2) A. J. McEvily: Metal Failures, John Wiley and Sons, New York, (2001), 1.
3) J. W. Morris, Jr., C. S. Lee and Z. Guo: *ISIJ Int.*, **43** (2003), 410. https://doi.org/10.2355/isijinternational.43.410
4) R. M. McMeeking and D. M. Parks: Elastic-Plastic Fracture, American Society for Testing and Materials, West Conshohocken, PA, (1979), 175.
5) G. Thomas: *Metall. Trans.*, **2** (1971), 2373. https://doi.org/10.1007/BF02814875
6) S. Takaki and T. Maki: Proc. Int. Symp. on Ultrafine Grained Steels (ISUGS-2001), ISIJ, Tokyo, (2001), 1.
7) Z. Guo, C. S. Lee and J. W. Morris, Jr.: *Acta Mater.*, **52** (2004), 5511. https://doi.org/10.1016/j.actamat.2004.08.011
8) Y. Kimura, T. Inoue, F. Yin and K. Tsuzaki: *Science*, **320** (2008), 1057. https://doi.org/10.1126/science.1156084
9) Y. Kimura, T. Inoue, F. Yin and K. Tsuzaki: *ISIJ Int.*, **50** (2010), 152. https://doi.org/10.2355/isijinternational.50.152
10) Y. Kimura and T. Inoue: *Metall. Mater. Trans. A*, **44** (2013), 560. https://doi.org/10.1007/s11661-012-1391-2
11) Y. Kimura and T. Inoue: *ISIJ Int.*, **55** (2015), 1135. https://doi.org/10.2355/isijinternational.55.1135
12) Y. Kimura, T. Inoue, T. Otani, A. Ochiai, S. Ikurumi and T. Takatsuji: *Mater. Sci. Eng. A*, **819** (2021), 141514. https://doi.org/10.1016/j.msea.2021.141514
13) A. Dolzhenko, Z. Yanushkevich, S. A. Nikulin, A. Belyakov and R. Kaibyshev: *Mater. Sci. Eng. A*, **723** (2018), 259. https://doi.org/10.1016/j.msea.2018.03.044
14) A. Dolzhenko, A. Pydrin, S. Gaidar, R. Kaibyshev and A. Belyakov: *Metals*, **12** (2022), 48. https://doi.org/10.3390/met12010048
15) A. S. Dolzhenko, P. D. Dolzhenko, A. N. Belyakov and R. O. Kaibyshev: *Phys. Met. Metallogr.*, **122** (2021), 1014. https://doi.org/10.1134/S0031918X21100021
16) A. Dolzhenko, R. Kaibyshev and A. Belyakov: *Materials*, **15** (2022), 5241. https://doi.org/10.3390/ma15155241
17) D. W. Kum, T. Oyama, J. Wadsworth and O. D. Sherby: *J. Mech. Phys. Solids*, **31** (1983), 173. https://doi.org/10.1016/0022-5096(83)90049-2
18) R. K. Ray, J. J. Jonas and R. E. Hook: *Int. Mater. Rev.*, **39** (1994), 129. https://doi.org/10.1179/imr.1994.39.4.129
19) H.-R. Wenk and P. V. Houtte: *Rep. Prog. Phys.*, **67** (2004), 1367. https://doi.org/10.1088/0034-4885/67/8/R02
20) T. Inoue, F. Yin, Y. Kimura, K. Tsuzaki and S. Ochiai: *Metall. Mater. Trans. A*, **41** (2010), 341. https://doi.org/10.1007/s11661-009-0093-x
21) A. Dolzhenko, R. Kaibyshev and A. Belyakov: *Metals*, **10** (2020), 1566. https://doi.org/10.3390/met10121566
22) Y. Kimura and T. Inoue: *ISIJ Int.*, **60** (2020), 1108. https://doi.org/10.2355/isijinternational.ISIJINT-2019-726
23) R. Mishnev, N. Dudova, R. Kaibyshev and A. Belyakov: *Materials*, **13** (2020), 3. https://doi.org/10.3390/ma13010003
24) T. Inoue, H. Qiu, R. Ueji and Y. Kimura: *Materials*, **14** (2021), 1634. https://doi.org/10.3390/ma14071634
25) X. Min, Y. Kimura, T. Kimura and K. Tsuzaki: *Mater. Sci. Eng. A*, **649** (2016), 135. https://doi.org/10.1016/j.msea.2015.09.102